Structures of strontium diformate and strontium fumarate. A synchrotron powder diffraction study

Kenny Ståhl,[a]* Jens E. T. Andersen,[a] Irene Shim[a] and Stephan Christgau[b]

[a]Chemistry Department, Technical University of Denmark, Building 207, DK-2800 Lyngby, Denmark, and [b]Osteologix A/S, Symbion Science Park, Copenhagen, Denmark

Correspondence e-mail: kenny@kemi.dtu.dk

The crystal structures of strontium diformate in space groups $P2_12_12_1$ (α form, 295 K), $P4_12_12$ (β form, 334 and 540 K) and $I4_1/amd$ (δ form, 605 K), and strontium fumarate in space groups $Fddd$ (β form, 105 K) and $I4_1/amd$ (α form, 293 K) have been determined from synchrotron X-ray powder diffraction data. Except for the α-strontium diformate, all the structures are based on a diamond-like Sr-ion arrangement, as in strontium acetylene dicarboxylate. The formate ions are disordered in the δ phase owing to steric hindrance. The fumarate ions are disordered over four (α) or two (β) symmetry-equivalent orientations. α-Strontium fumarate crystallizes with a unique 90° carboxylate dihedral angle, and is stable up to 773 K.
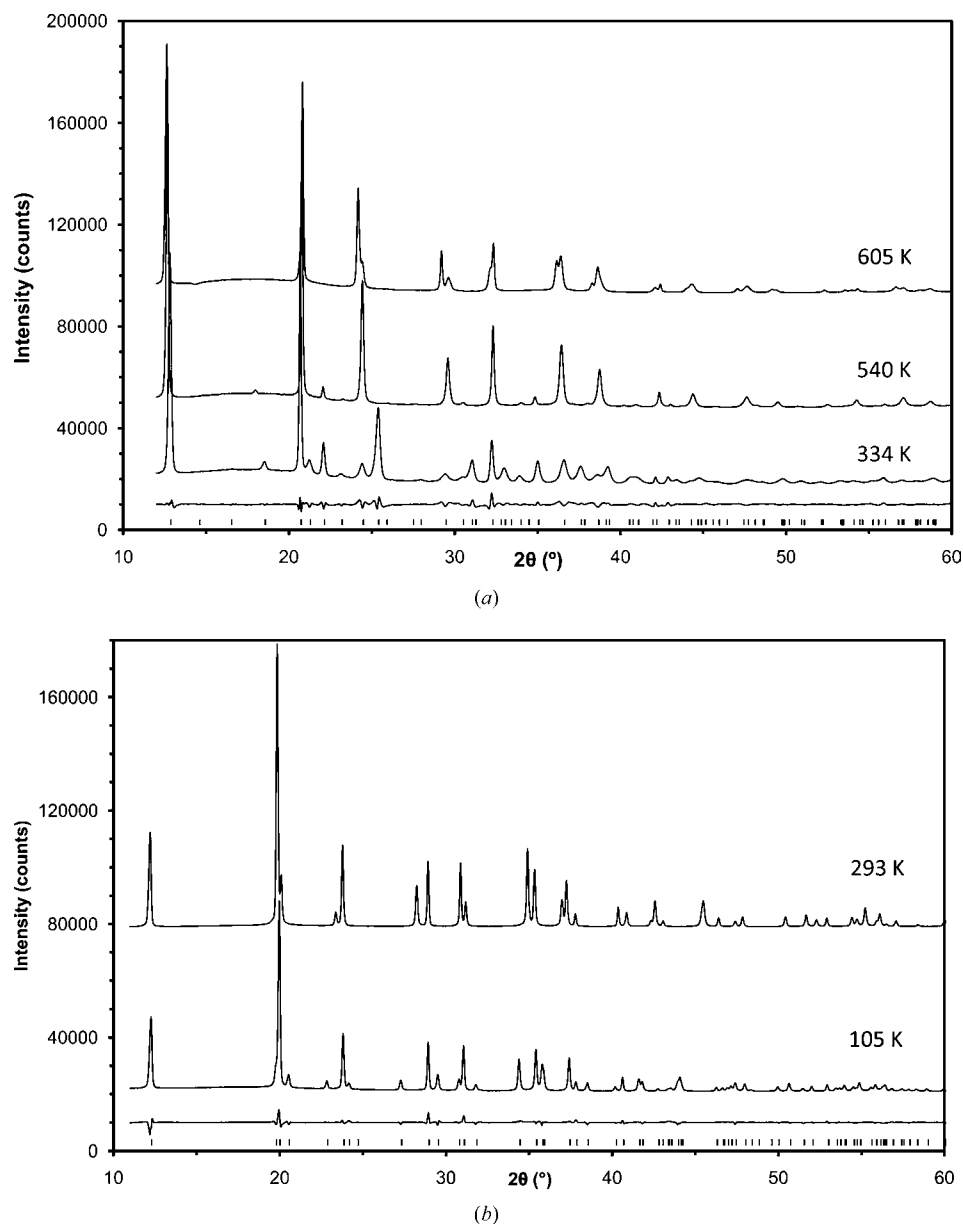
1. Introduction

Recent preclinical and clinical investigations have revealed that Sr^{2+} reduces bone re-sorption, while at the same time it provides a stimulus for new bone formation (Marie *et al.*, 2001). This combined action on bone metabolism sets Sr^{2+} apart from existing osteoporosis therapies and has lead to a growing interest in Sr^{2+} salts with different organic anions. Several organic strontium salts have recently been synthesized and structurally characterized by single-crystal methods (Christgau *et al.*, 2005; Stahl, Andersen & Christgau, 2006; Stahl, Andersen & Nilsson, 2006; Christgau *et al.*, 2006). However, some salts could not be produced as large enough crystals for single-crystal structure determination. One of those was strontium fumarate. From the first synthesis a powder diffraction database search-match identified the crystalline product as strontium diformate (Mentzen & Comel, 1974b). However, the strontium diformate search-match result referred to strontium diformate at 593 K in the space group $I4_1/amd$. At the same time a close similarity to the room-temperature powder diffraction pattern of strontium acetylene dicarboxylate (strontium ADC) was found, also in the space group $I4_1/amd$ (Hohn *et al.*, 2002). The three strontium salts were possibly isostructural. A Rietveld refinement of the strontium fumarate structure starting with the strontium and oxygen coordinates of strontium ADC (Hohn *et al.*, 2002) rapidly converged and the missing carbon positions (one ordered and one disordered) were located in a difference-Fourier map. Furthermore, the synthesis of strontium diformate dihydrate and consecutive heating to 593 K produced a powder diffraction pattern very similar to that of strontium fumarate. A Rietveld refinement starting from the strontium fumarate structure confirmed the structural similarity. Therefore, all three structures are isostructural in terms of their strontium carboxyl parts.

research papers

**Table 1**
Powder diffraction data collection and refinement overview.

	α-Sr(HCOO)$_2$ at 293 K	β-Sr(HCOO)$_2$ at 334 K	β-Sr(HCOO)$_2$ at 540 K
Crystal data			
Chemical formula	C$_2$H$_2$O$_4$Sr	C$_2$H$_2$O$_4$Sr	C$_2$H$_2$O$_4$Sr
M_r	177.66	177.66	177.66
Crystal system, space group	Orthorhombic, $P2_12_12_1$	Tetragonal, $P4_12_12$	Tetragonal, $P4_12_12$
Temperature (K)	293	334	540
a, b, c (Å)	6.86744 (3), 8.75087 (4), 7.26091 (3)	7.1358 (2), 7.1358 (2), 9.5908 (3)	7.09951 (7), 7.09951 (7), 10.0405 (1)
V (Å^3)	436.35 (1)	488.36 (2)	506.07 (1)
Z	4	4	4
Radiation type	Synchrotron	Synchrotron	Synchrotron
Radiation of incident radiation (Å)	1.28406 (1)	1.28406 (1)	1.28406 (1)
μ (mm^{-1})	9.63	8.60	8.30
Specimen shape, size (mm)	Cylinder, 2.0 × 0.3	Cylinder, 2.0 × 0.3	Cylinder, 2.0 × 0.3
Data collection			
Diffractometer	Huber G670 Guinier camera	Huber G670 Guinier camera	Huber G670 Guinier camera
Specimen mounting	Quartz capillary	Quartz capillary	Quartz capillary
Scan method	Step	Step	Step
Data-collection mode	Transmission	Transmission	Transmission
Absorption correction	For a cylinder mounted on the φ axis	For a cylinder mounted on the φ axis	For a cylinder mounted on the φ axis
T_{min}	0.327	0.354	0.354
T_{max}	0.368	0.397	0.397
2θ (°)	$2\theta_{min}$ = 12.005, $2\theta_{max}$ = 100.000, $2\theta_{step}$ = 0.005	$2\theta_{min}$ = 12.001, $2\theta_{max}$ = 100.006, $2\theta_{step}$ = 0.005	$2\theta_{min}$ = 12.006, $2\theta_{max}$ = 100.001, $2\theta_{step}$ = 0.005
Refinement			
Refinement on	I_{net}	I_{net}	I_{net}
R_p, R_{wp}, R_{exp}, R_B, χ^2	0.028, 0.038, 0.007, 0.023, 29.48	0.032, 0.050, 0.004, 0.013, 167.96	0.024, 0.036, 0.005, 0.009, 47.05
Profile function	Pseudo-Voigt	Voigt	Voigt
No. of data points	17 600	17 600	17 600
No. of Bragg reflections	472	289	298
No. of parameters	55	38	39
$(\Delta/\sigma)_{max}$	0.019	0.031	0.031

	δ-Sr(HCOO)$_2$ at 605 K	β-Sr(H$_2$C$_4$O$_4$) at 105 K	α-Sr(H$_2$C$_4$O$_4$) at 293 K
Crystal data			
Chemical formula	C$_2$H$_2$O$_4$Sr	C$_4$H$_2$O$_4$Sr	C$_4$H$_2$O$_4$Sr
M_r	177.66	201.68	201.68
Crystal system, space group	Tetragonal, $I4_1/amd$	Orthorhombic, $Fddd$	Tetragonal, $I4_1/amd$
Temperature (K)	605	105	293
a, b, c (Å)	7.0904 (1), 7.0904 (1), 10.1697 (2)	10.5980 (1), 9.81628 (9), 10.00739 (8)	7.24689 (5), 7.24689 (5), 10.01133 (7)
V (Å^3)	511.27 (1)	1041.10 (2)	525.77 (1)
Z	4	8	4
Radiation type	Synchrotron	Synchrotron	Synchrotron
Wavelength of incident radiation (Å)	1.28406 (1)	1.25176 (1)	1.25176 (1)
μ (mm^{-1})	8.21	7.58	7.51
Specimen shape, size	Cylinder, 2.0 × 0.3	Cylinder, 2.0 × 0.3	Cylinder, 2.0 × 0.3
Data collection			
Diffractometer	Huber G670 Guinier camera	Huber G670 Guinier camera	Huber G670 Guinier camera
Specimen mounting	Quartz capillary	Quartz capillary	Quartz capillary
Scan method	Step	Step	Step
Data-collection mode	Transmission	Transmission	Transmission
Absorption correction	For a cylinder mounted on the φ axis	For a cylinder mounted on the φ axis	For a cylinder mounted on the φ axis
T_{min}	0.354	0.423	0.423
T_{max}	0.397	0.452	0.452
2θ (°)	$2\theta_{min}$ = 12.002, $2\theta_{max}$ = 99.997, $2\theta_{step}$ = 0.005	$2\theta_{min}$ = 10.996, $2\theta_{max}$ = 99.996, $2\theta_{step}$ = 0.005	$2\theta_{min}$ = 10.997, $2\theta_{max}$ = 99.992, $2\theta_{step}$ = 0.005
Refinement			
Refinement on	I_{net}	I_{net}	I_{net}
R_p, R_{wp}, R_{exp}, R_B, χ^2	0.025, 0.041, 0.005, 0.020, 65.61	0.043, 0.059, 0.008, 0.034, 54.76	0.047, 0.064, 0.007, 0.035, 85.01
Profile function	Voigt	Pseudo-Voigt	Pseudo-Voigt
No. of data points	17 600	17 800	17 800
No. of Bragg reflections	137	147	147
No. of parameters	34	35	36
$(\Delta/\sigma)_{max}$	0.043	0.045	0.024

Computer programs used: Huber G670, *WINPOW*, local Rietveld program, *EXPO* (Altomare *et al.*, 1994, 1995), *ATOMS*6.2 (Dowty, 2002).

Figure 1
Powder diffractograms of strontium diformate, λ = 1.284065 (1) Å (top), and strontium fumarate, λ = 1.251760 (1) Å (bottom). The final Rietveld difference patterns of the 334 K (top) and 105 K (bottom) are shown at the bottom of the diagrams together with markers for the Bragg positions.
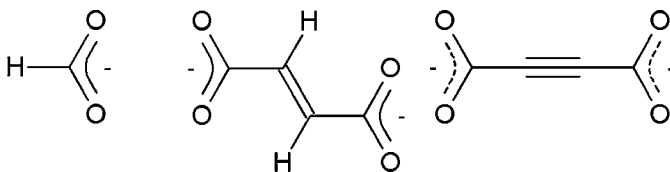
although some discrepancies exist between the published structures of the latter (Nitta & Saito, 1949; Watanabé & Matsui, 1978). Furthermore, the work by Mentzen & Comel (1974a) suggested two more strontium diformate phases: one tetragonal in the space group $P4_12_12$ and one cubic in the space group $F4_132$. Hohn *et al.* (2002) have clearly demonstrated that strontium ADC has no phase transitions between 30 K and its decomposition at 720 K. The purpose of the present work was to establish the stability range and possible phase transitions in strontium fumarate, and by means of X-ray powder diffraction to determine the crystal structures of the different phases of anhydrous strontium diformate and strontium fumarate.

2. Experimental methods

2.1. Syntheses

Sodium formate (7.658 g) was dissolved in 200 ml of distilled water and solid strontium chloride hexahydrate (15.01 g) was dissolved in 100 ml of distilled water. The solution of strontium was added to the stirred formate solution, and the white precipitate of strontium formate dihydrate formed with a total yield of 94%. Disodium fumarate (10 g) and strontium chloride hexahydrate (5 g) were each dissolved in 100 ml of water. The solution of strontium chloride was slowly added, under stirring, to the fumarate solution. A white precipitate of strontium fumarate formed with a total yield of 9.59 g.

2.2. Synchrotron X-ray powder diffraction data

Powder diffraction data were collected at Beamline I711 at the MAX-II synchrotron in Lund, Sweden (Cerenius *et al.*, 2000), using an Huber G670 Guinier imaging-strip camera (Ståhl, 2000). The high-temperature data were collected with a Huber G670.3 capillary furnace in the range 293–693 K, and the low-temperature data with an Oxford Cryosystem Cryojet in the range 105–293 K. The wavelengths 1.28406 (1) and 1.25176 (1) Å were determined using a Si standard. The high temperature was calibrated against the thermal expansion of a

The transformations between the different forms of strontium diformate have been studied by Comel & Mentzen (1994) and Mentzen & Comel (1974a). Only strontium diformate dihydrate (Galigné, 1971) and strontium diformate in the space group $P2_12_12_1$ have been structurally fully characterized,

Table 2
Interatomic distances (Å) and angles (°) in strontium diformate and strontium fumarate.

Compound	Sr(HCOO)$_2$	Sr(HCOO)$_2$	Sr(HCOO)$_2$	Sr(HCOO)$_2$	Sr(H$_2$C$_4$O$_4$)	Sr(H$_2$C$_4$O$_4$)
Form	α	β	β	δ	β	α
Space group	$P2_12_12_1$	$P4_12_12$	$P4_12_12$	$I4_1/amd$	$Fddd$	$I4_1/amd$
Temperature (K)	293	334	540	605	105	293
Sr—O1	2.538 (3)[i]	2.666 (5) [*2]	2.679 (5) [*2]	2.840 (2) [*4]	2.776 (1) [*4]	2.777 (1) [*4]
Sr—O2	2.691 (3)	2.932 (4) [*2]	2.963 (5) [*2]			
Sr—O3	2.673 (4)[ii]					
Sr—O4	2.718 (4)					
Sr—O1′	2.718 (3)	2.415 (3)[vi] [*2]	2.496 (4)[vi] [*2]	2.440 (2)[viii] [*4]	2.530 (1)[ix] [*4]	2.569 (1)[xi] [*4]
Sr—O2′	2.555 (2)[iii]	2.417 (4)[vii] [*2]	2.568 (5)[vii] [*2]			
Sr—O3′	2.645 (4)[iv]					
Sr—O4′	2.619 (4)[v]					
C1—O1	1.269 (5)	1.314 (8)	1.210 (9)	1.321 (4) [*2]	1.210 (2) [*2]	1.237 (2) [*2]
C1—O2	1.243 (5)	1.286 (8)	1.336 (10)			
O1—C1—O2	121.1 (3)	128.1 (5)	110.7 (6)	113.7 (5)	128.0 (3)	122.2 (2)
C2—O3	1.176 (7)					
C2—O4	1.216 (7)					
O3—C2—O4	125.7 (4)					
C1—C2					1.618 (4)	1.511 (3)
C2—C2′					1.289 (6)[x]	1.062 (5)[xii]

Symmetry codes: (i) $-x+\frac{3}{2}, -y+1, z-\frac{1}{2}$; (ii) $x+\frac{1}{2}, -y+\frac{1}{2}, -z+1$; (iii) $x+\frac{1}{2}, -y+\frac{3}{2}, -z+1$; (iv) $-x+1, y+\frac{1}{2}, -z+\frac{1}{2}$; (v) $-x+\frac{3}{2}, -y+1, z+\frac{1}{2}$; (vi) $-y+\frac{1}{2}, x-\frac{1}{2}, z+\frac{1}{4}$; (vii) $-y+\frac{1}{2}, x+\frac{1}{2}, z+\frac{1}{4}$; (viii) $-y+\frac{1}{4}, x-\frac{1}{4}, z+\frac{1}{4}$; (ix) $-x, y-\frac{1}{4}, z-\frac{1}{4}$; (x) $-x+\frac{1}{4}, y, -z+\frac{5}{4}$; (xi) $-x, y, z$; (xii) $-y+\frac{1}{4}, x+\frac{1}{4}, -z-\frac{1}{4}$.

Si standard (Okada & Tokumaru, 1984). The samples were contained in 0.3 mm quartz capillaries and data were accumulated for 5 min in the range 3–100° in steps of 0.05° in 2θ during constant spinning of the capillaries.

2.3. Structure solutions and refinements

Indexing and space-group determinations of powder patterns were all based on known unit cells (Nitta & Saito, 1949; Mentzen & Comel, 1974a; Hohn et al., 2002). The crystal structure of strontium diformate in the space group $P2_12_12_1$ at 293 K was solved with *EXPO* (Altomare et al., 1994, 1995). The remaining structures were solved starting from the strontium and oxygen positions of strontium ADC (Hohn et al., 2002) and locating the missing carbon positions from difference-Fourier maps. H atoms were added in calculated positions in all of the structures with C—H distances of 0.90 Å. The Rietveld refinements (Rietveld, 1969) utilized a locally
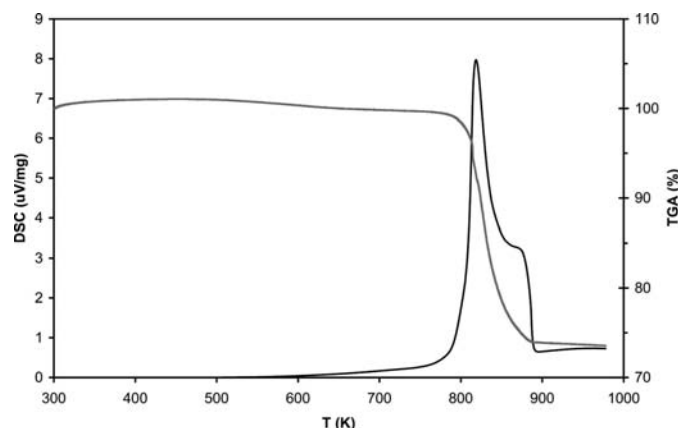
Figure 2
TGA (gray) and DSC (black) curves from strontium diformate.
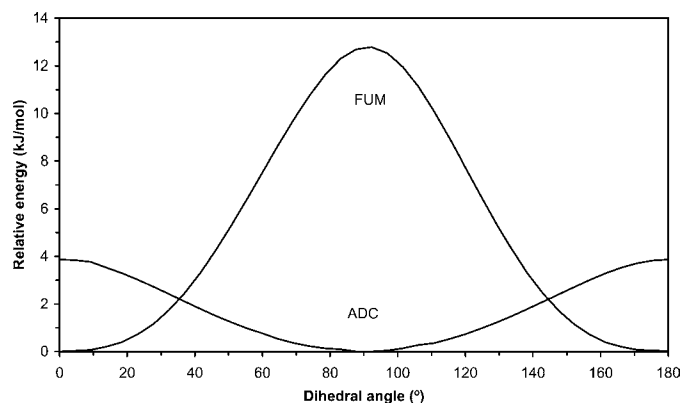
Figure 3
Rotational barriers in the fumarate (FUM) and acetylene dicarboxylate (ADC).

modified and Windows-adapted version of the *LHMP* program (Howard & Hill, 1986). The parameter set included: 2θ zero and Chebyshev background; pseudo-Voigt or Voigt half-width, peak shape, asymmetry and preferred orientation; and scale factor, unit cell, fractional coordinates and displacement parameters. Two isotropic isplacement parameters were refined for each structure, one for the Sr ions and one for all the C and O atoms. A data collection and refinement summary is given in Table 1,[1] selected diffractograms are shown in Fig. 1, the final atomic parameters have been deposited, and a selection of distances and angles are given in Table 2. It should be pointed out that the relatively high goodness-of-fits (5.40–12.93) are a consequence of the systematic nature of the peak misfits in combination with the very high intensities obtained from the synchrotron.

---

[1] Supplementary data for this paper are available from the IUCr electronic archives (Reference: ZB5005). Services for accessing these data are described at the back of the journal.

2.4. TGA/DSC

TGA (thermogravimetric analysis) and DSC (differential scanning calorimetry) measurements on strontium fumarate were performed on a Netsch STA 409 PC with a 22.9 mg sample between 293 and 973 K at 10 K min^{-1} and in an air flow of 20 ml min^{-1}. The resulting curves are shown in Fig. 2.

2.5. Theoretical calculations

The rotational barriers around the C—C single bonds in both the fumarate and acetylene dicarboxylate ions have been investigated by optimizing the geometry subject to constraining the appropriate dihedral angle in MP2 calculations using the basis set 6-311-G**. The calculations were performed using *Spartan*'06 (Wavefunction Inc., 2006). The

resulting curves are shown in Fig. 3. The (carboxylate) dihedral angle is defined as the angle between the normals to the two carboxyl O—C—O planes.

3. Results

3.1. Strontium diformate

The crystal structure after dehydration, α-Sr(HCOO)$_2$, is essentially as described by Watanabé & Matsui (1978) in the space group $P2_12_12_1$, which differs in the C position compared with Nitta & Saito (1949; see Fig. 4a and supplementary material). On heating to 527 K the α phase transforms to δ-Sr(HCOO)$_2$, space group $I4_1/amd$ (Fig. 4c and supplementary material). In the δ phase the ideal C1 position, 8e, $0\,\frac{1}{4}\,z$, was
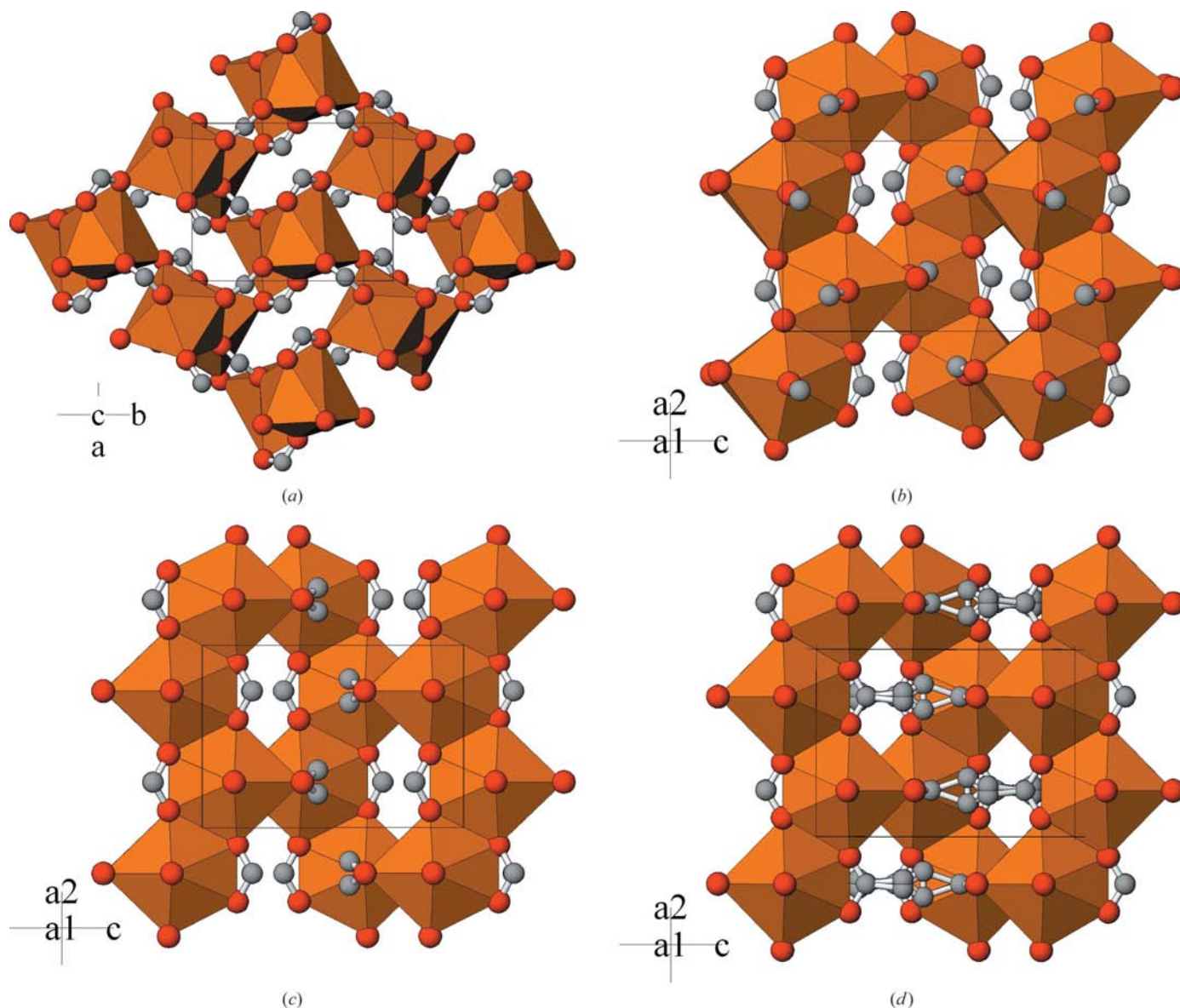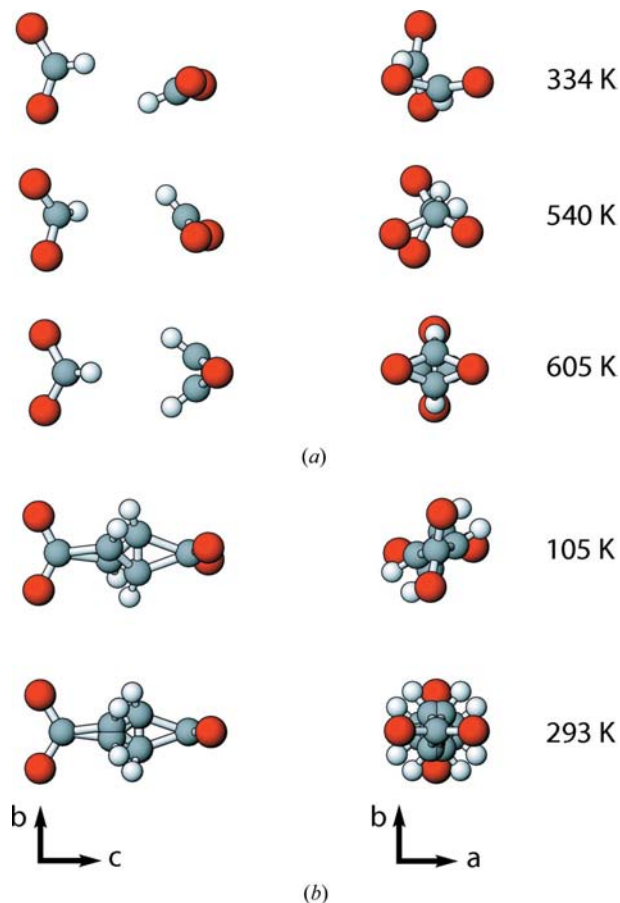

Figure 4
(a) Projection of α-strontium diformate in the space group $P2_12_12_1$ at 293 K. (b) Projection of β-strontium diformate in the space group $P4_12_12$ at 334 K. (c) Projection of δ-strontium diformate in the space group $I4_1/amd$ at 605 K. (d) Projection of α-strontium fumarate in the space group $I4_1/amd$ at 293 K. Sr^{2+} ions are at the centers of the orange polyhedra, O atoms are red, C atoms are grey and H atoms are omitted.

found split into two randomly occupied, 16h, 0 y z, sites. If the idealized site were occupied the distance between adjacent C atoms would be 3.674 (9) Å. Adding the H atoms with C—H distances of 1.05 Å would result in H—H distances of 1.574 Å, much shorter than twice their van der Waals radii. The C1 disordering thus allows for tolerable H—H distances (Fig. 5). With cooling down to 502 K the δ phase transformed to yet another phase, β-Sr(HCOO)$_2$, where ordering of the formates reduces the space-group symmetry to $P4_12_12$ (supplementary material). The β phase is retained with further cooling to 334 K (Fig. 4b and supplementary material). On cooling to room temperature the β phase is initially retained, but it transforms back to the α phase within a few minutes. We had wanted to follow this sequence of transformations in more detail. However, owing to radiation damage it was only possible to record two datasets per sample (maximum 10 min in the beam) before peak broadening and low intensity spoiled the powder patterns and data interpretation.

3.2. Strontium fumarate

The 293 K structure is very similar to the strontium ADC structure; as in the ADC, the carboxylate dihedral angle is 90°. Owing to the site symmetry the double-bonded C atoms 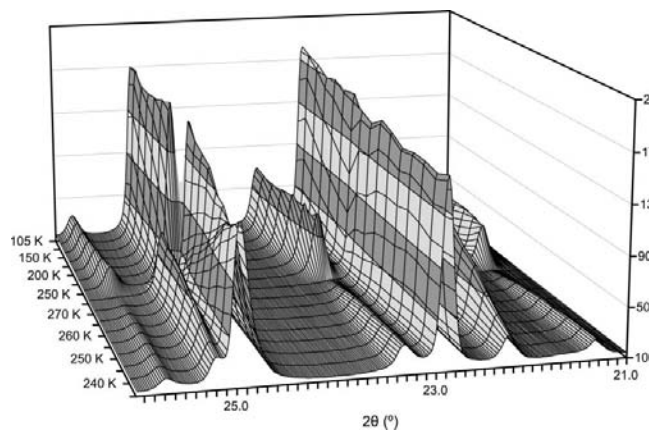and corresponding H atoms in the fumarate are disordered, at 293 K into four and at 105 K into two alternative sites. On heating to 673 K the strontium fumarate structure showed continuous increases in both the a and c axes, but without signs of any phase transitions. Neither did the TGA/DSC measurements indicate any phase transitions until the final breakdown starting at approximately 773 K (Fig. 2). However, on cooling to 105 K strontium fumarate transformed to an orthorhombic phase in the space group $Fddd$. On slow heating it transforms back to tetragonal between 250 and 270 K. On repeated cooling the transformation appeared gradually with a coexistence of the two phases between 293 and 200 K (Fig. 6). Tentatively, the transition temperature can be estimated to be 260 ± 5 K based on the heating experiment.

4. Discussion

4.1. Strontium diformate

In δ-strontium diformate the ordered H sites are too close in the c direction, which force a displacement of the C and H sites in the a and b directions. When the C and H sites become ordered in the β phase it allows for a contraction of the c axis by 5.7% between 605 and 334 K, accompanied by a minor expansion in the a and b axes of 0.5%. During this lattice contraction the c/a ratio continuously changes from 1.434 to 1.344, thereby passing $2^{1/2}$ and a face-centered pseudo-cubic setting ($a' = a + b$ and $b' = a - b$). It was suggested by Mentzen & Comel (1974a) that the structure having $c/a = 2^{1/2}$ represented a true cubic δ-phase, and appears as such in the JCPDS-ICDD record 28-1218. However, this is just a metric coincidence. Even though the Sr ions adopt a diamond lattice, the formate arrangement does not allow for an overall cubic symmetry. The β-phase appears only after the initial transformation of the α phase to the δ phase, *i.e.* β-Sr(HCOO)$_2$ is metastable. Contrary to the order–disorder type δ to β transformation, the β to α and α to δ transformations require a rearrangement of the connectivity (*cf.* Figs. 4a–c). The transformation to the low-temperature α-phase is accompanied by

Figure 5
Diformate and fumarate conformations in (a) strontium diformate at 334, 540 and 605 K, and (b) strontium fumarate at 105 and 293 K.

Figure 6
Sections of powder diffraction patterns collected for strontium fumarate in the sequence 105–125–150–175–200–225–250–275–270–265–260–255–250–245–240–235 K.

a large increase in density, 11.9%, which can be considered as the driving force for this phase transformation.

4.2. Strontium fumarate

In α-strontium fumarate, the fumarate shows an unusual carboxylate dihedral angle of 90° despite an energy loss of 13 kJ mol^{-1} relative to a planar conformation (Fig. 3). This is in contrast to the ADC conformation in strontium ADC (Hohn *et al.*, 2002), where the 90° dihedral angle corresponds to the energy minimum (Fig. 3). In fact, a 90° carboxylate dihedral angle is unique for fumarate and fumaric acid derivatives: A search of the Cambridge Structural Database (CSD; Allen, 2002) resulted in 322 structures containing fumarates, fumaric acid or derivatives thereof; only four have a dihedral angle of 90°, and they all have either altered conjugation schemes by substitutions and/or coordination. Among pure fumarates, hydrogen fumarates or fumaric acids only very few showed deviations from planar conformation and then by a maximum of 30°. On the other hand, the strained conformation in strontium fumarate explains the existence of the low-temperature β-phase simply as an attempt to reduce the conformational strain. The dihedral angle at 105 K is 76°, increasing to 77° at 250 K, corresponds to an energy gain of ~ 2 kJ mol^{-1}.

The a/b ratio at 105 K of 1.08 is most likely the reason for the sluggish α to β transformation on cooling. This large difference will create strain in the material during the phase transformation, which will hamper the completion of the transformation (*cf.* for instance, the martensitic transformation in carbon steel).

5. Conclusions

The similarities in the powder diffraction patterns of strontium ADC, strontium fumarate and the high-temperature δ phase of strontium diformate is explained by the their very similar structures based on a diamond-like Sr-ion arrangement (Hohn *et al.*, 2002). A variable-temperature powder diffraction study has clarified the phases present in the strontium diformate and fumarate systems:

(i) Strontium diformate shows two stable phases: The α phase ($P2_12_12_1$) stable up to 508 K; and the δ phase ($I4_1/amd$) stable from 508 to 633 K, where $SrCO_3$ formation starts (Mentzen & Comel, 1974*a*). On cooling the δ phase a metastable β phase ($P4_12_12$) is formed, which can be maintained until room temperature. The δ phase is disordered in the formate C—H part for steric reasons, while the β phase is fully ordered. There is no true cubic phase.

(ii) *Strontium fumarate* shows two stable phases: The α phase ($I4_1/amd$) is stable between 260 and 800 K; the β phase (*Fddd*) is stable below 260 K. The fumarate ions crystallize in the α phase with the most unfavorable carboxylate dihedral angle of 90°, which is slightly reduced, to 76°, in the β phase at 105 K. The 90° dihedral angle is unique among known fumarate structures. The fumarate ions are disordered over four equivalent orientations in the α phase, and over two orientations in the β phase. α-Sr fumarate is stable to approximately 773 K.

References

Allen, F. H. (2002). *Acta Cryst.* B**58**, 380–388.
Altomare, A., Burla, M. C., Cascarano, G., Giacovazzo, C., Guagliardi, A., Moliterni, A. G. G. & Polidori, G. (1995). *J. Appl. Cryst.* **28**, 842–846.
Altomare, A., Cascarano, G., Giacovazzo, C., Guagliardi, A., Burla, M. C., Polidori, G. & Camalli, M. (1994). *J. Appl. Cryst.* **27**, 435.
Cerenius, Y., Ståhl, K., Svensson, L. A., Ursby, T., Oskarsson, Å., Albertsson, J. & Liljas, A. (2000). *J. Synchrotron Rad.* **7**, 203–208.
Christgau, S., Odderhede, J., Stahl, K. & Andersen, J. E. T. (2005). *Acta Cryst.* C**61**, m259–m262.
Christgau, S., Ståhl, K. & Andersen, J. E. T. (2006). *J. Coord. Chem.* **59**, 2023–2030.
Comel, B. & Mentzen, B. F. (1974). *J. Solid State Chem.* **9**, 210–213.
Dowty, E. (2002). *ATOMS*, Version 6.2. Shape Software, Kingsport, Tennessee, USA.
Galigné, J. L. (1971). *Acta Cryst.* B**27**, 2429–2431.
Hohn, F., Pantenburg, I. & Ruschewitz, U. (2002). *Chem. Eur. J.* **8**, 4536–4541.
Howard, C. J. & Hill, R. J. (1986). AAEC (now ANSTO), Report M112. Lucas Heights Research Laboratory, Australia.
Marie, P. J., Ammann, P., Boivin, G. & Rey, C. (2001). *Calcif. Tissue Int.* **69**, 121–129.
Mentzen, B. & Comel, B. (1974*a*). *J. Solid State Chem.* **9**, 214–223.
Mentzen, B. & Comel, B. (1974*b*). JCPDS-ICDD Powder pattern 28–1218.
Nitta, I. & Saito, Y. (1949). *X-rays*, **5**, 89–94.
Okada, Y. & Tokumaru, Y. J. (1984). *Appl. Phys.* **56**, 314–320.
Rietveld, H. M. (1969). *J. Appl. Cryst.* **2**, 65–71.
Ståhl, K. (2000). *J. Appl. Cryst.* **33**, 394–396.
Stahl, K., Andersen, J. E. T. & Christgau, S. (2006). *Acta Cryst.* C**62**, m144–m149.
Stahl, K., Andersen, J. E. T. & Nilsson, H. (2006). *Acta Cryst.* E**62**, m1677–m1679.
Watanabé, T. & Matsui, M. (1978). *Acta Cryst.* B**34**, 2731–2736.
Wavefunction Inc. (2006). *Spartan*'06. Wavefunction Inc. Irvine, CA.